Effects of temperature and slope on the infiltration rate for a landfill surface

Lohit Jain* and Sumedha Chakma

Department of Civil Engineering, Indian Institute of Technology, Delhi 110 016, India

In this study, parameters of the Kostiakov, Horton, Modified Kostiakov, SCS, Philip and Smith models were estimated using the double-ring infiltrometer on two different slopes, viz. 4° and 23°; in morning and afternoon sessions to assess their usefulness in characterizing the infiltration process. Observations revealed that the average increment in temperature by 9°C increased the final and initial infiltration rates by 65% and 38% respectively. The combined effects of the 23° slope and higher temperature increased the infiltrated volume by 6.4 times. The comparative analysis showed Kostiakov as the most efficient model incorporating combined and individual effects of temperature and slope.

Keywords: Double-ring infiltrometer, infiltration rate, landfill, slope, temperature.

THE rapid growth of industries has led to the migration of people from villages and towns towards the urban, causing rapid population growth in metro cities and resulting in a large amount of solid waste generation[1]. The population in Delhi, India has increased from 13.9 million in 2001 to 16.8 million in 2011 and 30.3 million in 2020 (ref. 2). This has increased the solid waste generation from 1.05×10^4 TPD (tonnes per day) in 2016 to 1.11×10^4 TPD in 2021 (refs 3 and 4). Primarily, three landfill sites, viz. Gazipur, Bhalswa and Okhla were chosen for dumping solid waste over a total area of 60 ha in Delhi[5]. The present study highlights the infiltration characteristics of the Okhla landfill, incorporating slope and temperature variations. The Okhla landfill processes approximately 1800 TPD, which was 51% of the total solid waste generation (3600 TPD) in South Delhi in 2019–20 (ref. 6). Dumping of solid waste is poorly managed, and this has generated a massive mountain of waste of 40 m height, against the permissible limit of 20 m with a spread of 46-acre area of solid waste[6].

The landfill is a heterogeneous system where infiltration is one of the prime causes of leachate generation[7]. The generated leachate significantly affects the hydraulic conductivity of the soil system, groundwater quality and nitrogen diminution[8]. It is established that field density, temperature variation, moisture content of the top surface and type of waste are the main factors influencing the infiltration process and leachate generation[9,10].

Several experiments have been conducted on the suitability of the different models by comparing the model output and field observations[11,12]. In a field study, the dependency of the steady-state infiltration rate showed weak correlations with textural variables and a strong correlation with the structural arrangement of the soil particles[13]. In the last century, many physical, semi-empirical and empirical infiltration models have been developed[14]. The previous study reported that the infiltration rate was underestimated by the Philip (PH) model for the time beyond the experiment duration; however, steady-state infiltration rates predicted by the Horton (HO) model are reported to be fairly accurate[15]. Model preciseness depends on soil characteristics, land-use land-cover, temperature variation, slope and initial moisture content[16–19].

The effects of temperature variation and different surface inclinations were considered the governing factors for the infiltration experiments. Experimental data and theoretical studies have shown that temperature and slope of the surface significantly influence the hydrologic processes and infiltration mechanism, which have not been considered in classical infiltration models for any land use[20]. Infiltration is such a complex physical phenomenon that no single model has been found suitable for all the temperature ranges and slopes; hence it is difficult to identify the most appropriate model for a given condition[21].

Infiltration models

Various mathematical expressions have been proposed for describing the one-dimensional infiltration process. Some of the most common models were calibrated to study the effects of slope and temperature variation on the infiltration model parameters for the municipal solid waste landfill in Okhla (Table 1). The objective of this study was to examine the individual and combined impact of diurnal temperature variation and slope on the infiltration process for the municipal solid waste landfill as well as variation in the parameters of six popular infiltration models for focused factors (slope and temperature). We also did a comparative analysis of the outcome of the classical infiltration models to evaluate their suitability for the given slope and temperature variation conditions.

*For correspondence. (e-mail: cez148040@civil.iitd.ac.in)

Table 1. Classical infiltration models and parameters[12,14]

Infiltration model	Equations	Parameters
Kostiakov model	$f = \alpha t^{\beta}$, $F = at^{b}$	F is the cumulative infiltration, a a constant and b is a dimensionless positive exponent less than one. f is the infiltration rate at time t. $\alpha = ab$ and $\beta = b - 1$.
Horton model	$f_t = f_c + (f_o - f_c)e^{-kt}$	f_t is the infiltration rate at time t, f_o the initial infiltration rate (at $t = 0$), f_c the final constant infiltration, k a model parameter and t is the elapsed time. k is the decay constant that depends on the soil characteristics and surface cover.
Modified Kostiakov model	$f_t = f_c + \alpha t^{\beta}$	f_t is the infiltration rate at time t, α and β are constants.
SCS model	$F(t) = at^{b} + 0.6985$	a and b are the equation constants, and F is the cumulative infiltration rate.
Philip model	$f(t) = \frac{1}{2}st^{-1/2} + A$ $F(t) = st^{1/2} + At$	$F(t)$ is the cumulative infiltration till elapsed time t. $f(t)$ is the infiltration rate, where s the sorptivity, A the Philip model constant and t is the elapsed time for infiltration.
Smith model	$f(t) = f_c + A(t - t_o)^{-b}$	t_o is the time when run-off started, A a constant and b is an exponent depending on other factors governing the infiltration process, such as soil characteristics, moisture content and rainfall intensity.

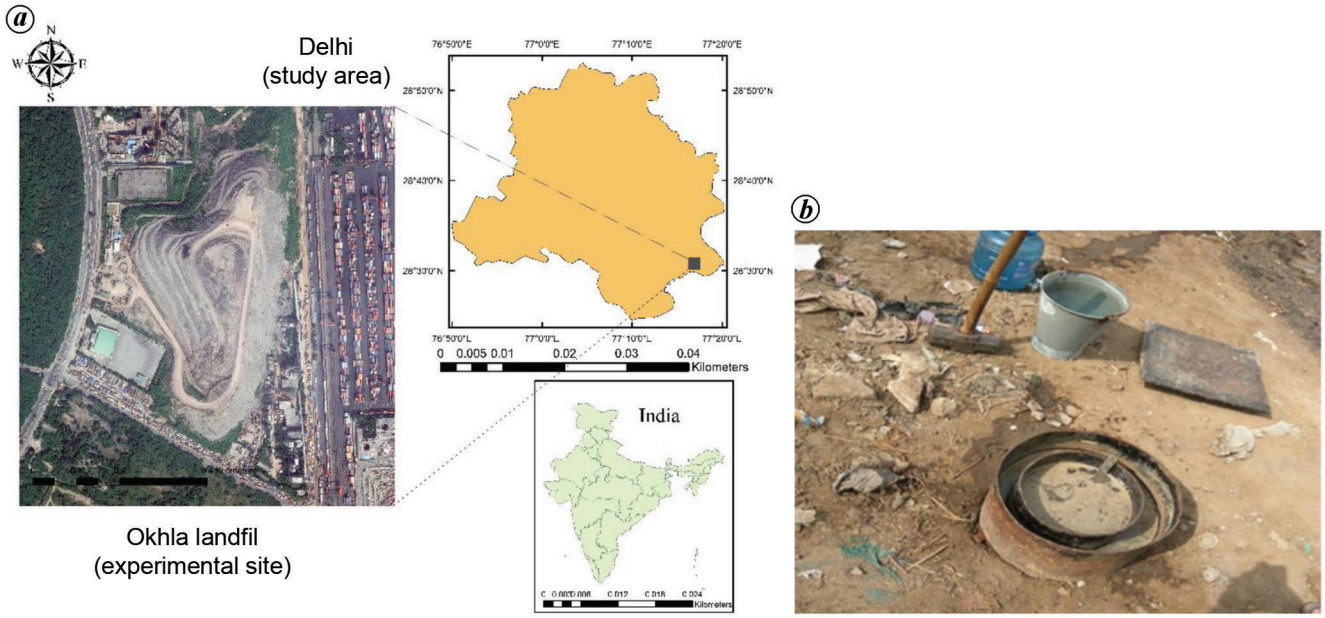

Figure 1. ***a***, Location of the study area. ***b***, Experimental set-up at Okhla landfill, Delhi, India.

Materials and method

Study area

Delhi is the capital of India, covering a 1483 sq. km area. In the last 14 years, the highest annual rainfall was recorded as 1530 mm in 2013, and the yearly minimum rainfall as 560 mm in 2012, with an average rainfall of 880 mm (ref. 22). Delhi has a subtropical climate, where the summers are very hot with temperatures reaching 45°C and winters are very cold with temperatures falling to 2°C. The annual average difference in maximum and minimum diurnal temperature in Delhi has been observed to be approximately 11°C (ref. 23).

The present study was conducted at a non-engineered municipal solid waste landfill in Okhla (Figure 1 *a*) using a double-ring infiltrometer (Figure 1 *b*). The Okhla landfill site was commissioned in 1994 and is owned by South Delhi Municipal Corporation for dumping solid waste. The dumped municipal waste was covered by a 45–60 cm thick soil layer to obstruct direct exposure to the atmosphere[24].

Field experiment

The ring infiltrometer is the most common instrument for measuring cumulative infiltration on the field[25]. Three sets of ring-infiltrometer experiments were performed at the Okhla landfill during April–May 2016 on a plain surface (4°) and slope (23°) in the afternoon and morning sessions for 3.5–4 h to incorporate the effect of diurnal temperature variation on the infiltration mechanism. The procedure of

double-ring infiltrometer experiments, as mentioned in the American Society for Testing and Materials (ASTM) manual, was followed[26]. The prime advantage of ring-infiltrometers is the feasibility of field experiments without conserving and collecting the samples from the site at an economical cost and lesser water consumption than rainfall simulators[27]. Dimensions of 45 × 30 × 30 cm for the outer infiltrometer ring diameter, inner ring diameter and height of the rings were used for the field experiments under the following four conditions: (a) plain surface in the morning session (4° slope, 26–32°C), (b) plain surface in the afternoon session (4°, 36–42°C), (c) inclined surface in the morning session (23° slope, 30–35°C) and (d) inclined surface in the afternoon session (23° slope, 38–42°C). Experiments were performed under all the above-mentioned conditions to observe the effect of temperature (condition b), slope (condition c) and the combination of slope and temperature (condition d) compared to condition a. The temperature was measured near the surface using a calibrated digital temperature meter (model no. PW18183, Sigma, Series-HTC-1) for each infiltration observation. The ring was installed at approximately 5 cm depth in the upper layer of the soil by hammering the tray laid over the ring for uniform impact. Observations were made at variable intervals from 30 to 1800 sec based on the constant infiltration rate attained for each interval. Water was replenished with minimum turbulence after its level fell about 4–5 cm in the ring. In the double-ring experiment, the water level was kept the same in both rings for effective vertical infiltration. The experiment was carried out until a constant infiltration rate was obtained during observations at 30 min intervals. Table 2 presents the initial infiltration rate (f_o, cm/min), final infiltration rate (f_c, cm/min), slope and temperature (°C) ranges during experiments in the Okhla landfill.

The waste samples were collected from a 20 cm depth near the study area, as suggested by Shukla[28]. The double-ring infiltrometer was hammered up to 5 cm in the ground to minimize soil disturbance[29]. The soil matrix of 0–20 cm depth plays a significant role in the orientation of the infiltration process. Experimental observations were made using soil characteristics from the top 20 cm; therefore, sampling from variable depth was not chosen. Three sets of particle size distribution, initial moisture content, specific gravity, liquid limit, plastic limit, falling head permeability and standard proctor experiments in the laboratory and core-cutter test in the field were performed to analyse the physical and hydraulic characteristics of the soil. The samples were carried from the field to the laboratory and stored in airtight bags to preserve moisture. Soil particle distribution was studied using sieve analysis (coarse particles) and a hydrometer (fine particles). Totally 3.3% weight of the soil sample was lost during the experiments. Average soil characteristics were measured experimentally (Table 3).

For the Okhla landfill, variations of different types of density, porosity and void ratio were evaluated (Figures 2 and 3).

Performance assessment

Nash–Sutcliffe efficiency (NSE), coefficient of determination (R^2), per cent bias (PBIAS) and root mean square error observations standard deviation ratio (RSR) were selected for model assessment and experimental comparison in the infiltration process for different scenarios[30].

If x-series and y-series represent the observed and simulated infiltration values respectively, and $\bar{x}$ is the mean value for the same series, NSE can be evaluated using eq. (1)

$$\mathrm{NSE} = 1 - \left[\frac{\sum_{i=1}^{n} (x - y)^2}{\sum_{i=1}^{n} (x - \bar{x})^2} \right]. \quad (1)$$

R^2 explains the percentage variation in the simulated infiltration rate and infiltrated amount with respect to the observed results in terms of the degree of collinearity (eq. (2))[31].

Table 2. Average initial and final infiltration rates for different scenarios

Case	f_o (cm/min)	f_c (cm/min)	Slope (°)	T (°C)
1	0.2	0.01	4	26–32
2	0.2	0.02	4	36–42
3	0.4	0.02	23	30–35
4	0.4	0.05	23	38–42

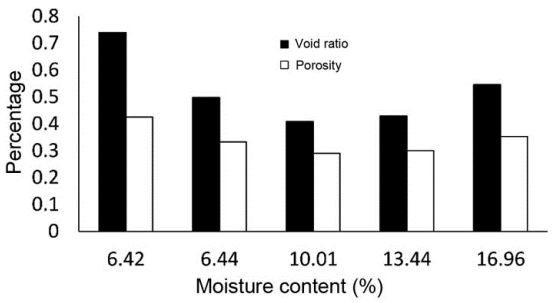

Figure 2. Porosity and void ratio variations with increasing moisture content for the Okhla top-layer soil.

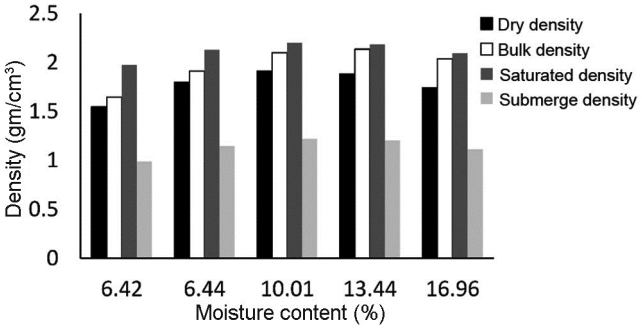

Figure 3. Density variation with moisture content for the top surface layer of the landfill.

Table 3. Okhla landfill, Delhi, India, top-layer average soil characteristics at moisture content of 6.4%

Soil characteristics	Measured average value (three sets)
Average field density on natural moisture content	1.64 g/cm^3
Liquid limit	20.69%
Specific gravity	2.63
Soil type (from 0 to 20 cm depth)	Silty sand (gravel = 20.37%, sand = 59.26%, silt = 14.32%, clay = 2.73%)
Maximum dry density	1.916 g/cm^3 at 11% moisture content
Saturated hydraulic conductivity	6.85×10^{-3} cm/min

$$R^2 = \left[\frac{\sum_{i=1}^{n} (x - \bar{x})(y - \bar{y})}{\sum_{i=1}^{n} (x - \bar{x})^2 \sum_{i=1}^{n} (y - \bar{y})^2} \right]^2. \quad (2)$$

PBIAS was computed using eq. (3), which measures the difference between the model infiltration rate and the corresponding experimental values[31].

$$\text{PBIAS} = \frac{\sum_{i=1}^{n} (x - \bar{y}) 100}{\sum_{i=1}^{n} x}. \quad (3)$$

RSR was calculated using eq. (4), which has the advantages of error index statistics and incorporates a normalizing factor; so the resulting statistics and reported values can apply to different output responses[31].

$$\text{RSR} = \left[\frac{\sum_{i=1}^{n} (x - y)^2}{\sum_{i=1}^{n} (x - \bar{x})^2} \right]. \quad (4)$$

Results

The observed experimental datasets from each scenario for a duration of 3–4 h were used to generate and analyse the infiltration rate curves. Figure 4 summarizes the results of the observed infiltration rates in different scenarios. The initial infiltration rate showed no noticeable change from 26°C to 32°C (morning session) and 36–42°C (afternoon session). However, the final infiltration rate showed proportionality with the mentioned temperature ranges on the plain surface, yet it did not present any significant correlation. On the other hand, as the slope increased from plain surface to 23° inclination, the initial–final infiltration rates increased approximately two times under ponded conditions (Table 2), which is equivalent to the final infiltration rate ratio of 1.9 for the diurnal temperature variation from 14.9°C to 31.5°C (ref. 32). Similar results were observed

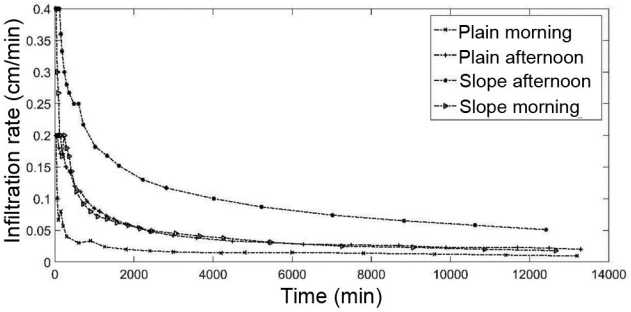

Figure 4. Observed infiltration rate for different slopes and temperature variations in the Okhla landfill.

at the 10°slope for loamy sand, 30° slope for sandy loam and 23° slope for silty loam because of the influence of surface roughness and micro-relief features[33–35].

The infiltrated volume was approximately twice in the afternoon session with a temperature range 36–42°C compared to the morning session with a temperature range 26–32°C for the plain surface. Cumulative infiltration for the experiment on a 23° slope surface was observed to be 1.6 and 2.3 times higher than the plain surface under the temperature conditions of the morning and afternoon sessions respectively. The cumulative infiltration was 4.6 times higher for the combined effect of higher temperature and slope than the total infiltrated volume on the plain surface in the morning session (Table 2).

Some classical infiltration models were evaluated to analyse the field infiltration experiments at the Okhla landfill. HO, Kostiakov (KO), Smith (SM), PH, modified Kostiakov (MK) and SCS were selected to estimate model parameters using the observed field infiltration data. The estimated infiltration values from each focused model were compared with the observed data to identify the best-suited model for inclined and plain surfaces, as shown in Figures 5 and 6 respectively.

All the chosen models were fitted to the observed data from infiltration experiments using a nonlinear least square technique with the GRG nonlinear method for infiltration rate curves. Analysis of the curves for the combined impacts of slope and the higher temperature (Figure 5 *a*) showed that the MK model was the most efficient for infiltration rate in this scenario by delivering optimum values of statistical parameters (Table 4). The HO model estimated the infiltration rate reasonably well at the start and end of the process

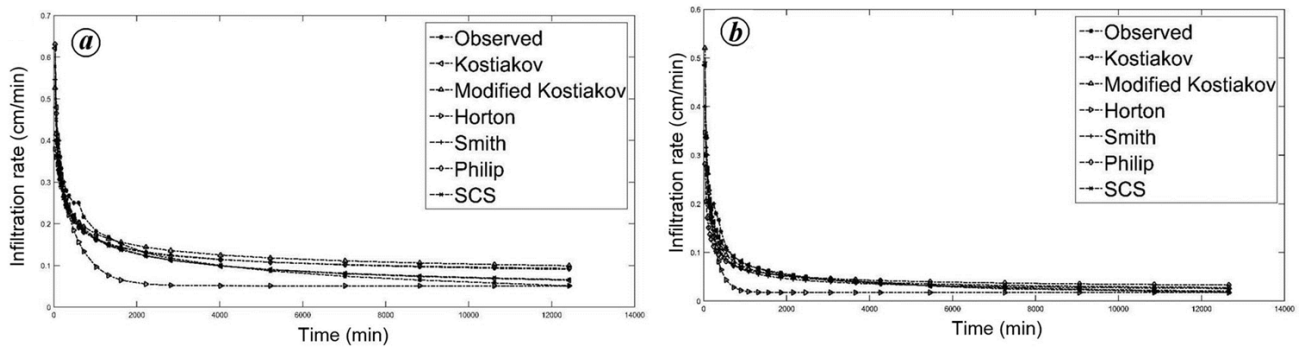

Figure 5. ***a***, Comparative curves of infiltration rate for slope of 23° and temperature variation from (***a***) 38°C to 42°C and (***b***) 30°C to 35°C.

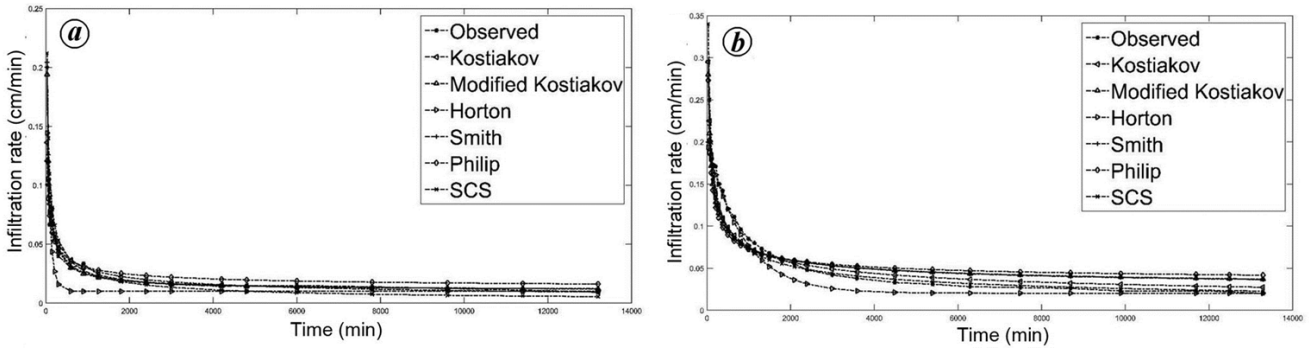

Figure 6. Comparative curves of infiltration rate for slope of 4° and temperature variation from (***a***) 26°C to 32°C and (***b***) 36°C to 42°C.

but showed a significant difference from the observed data after 10 to 100 min (Figure 5 *a*). The PH model gave the poorest results for estimating initial–final infiltration rates in this scenario among all the models; yet it performed better for cumulative infiltration estimation in the same field conditions. The KO model was the most efficient for estimating cumulative infiltration in this scenario.

Analysis of the classical models for the combined impact of slope and higher temperature was done in the performance order KO > PH > SCS > HO > MK > SM.

Infiltration rate curves for 23° inclined surfaces in the morning session were generated to analyse the effect of slope (Figure 5 *b*). It is evident from the statistical comparison in Table 4 that the KO and SCS models estimated infiltration rates closer to experimental values than the other models for 23° inclined surface with a lower temperature range (Figure 5 *b*), as the variation of initial and final infiltration rate was observed to be 20% and 11% respectively. The PO model performed poorly in this situation and underestimated the initial infiltration rate by 29%. The performance of the other model was 'satisfactory to good' for estimating cumulative infiltration on the inclined surface during the morning session in the performance order KO > MK > SCS > HO > SM > PH.

In the morning session on the plain surface, all models slightly overestimated the initial infiltration rates (Figure 6 *a*), except for the SM and SCS models. The performance of the models was found to be better for plain surfaces and lower temperature range compared to the other three scenarios, although the KO and HO models outperformed the others in this scenario and estimated the results closest to the field experimental values. In the afternoon session, all the models overestimated the cumulative infiltration for the plain surface, whereas the KO model performed relatively better by showing less variation from the observed values. Analysis was conducted to estimate infiltration rate curves in the same scenario, where the KO and HO models presented better results than the others (Figure 6 *b*). From the statistical comparison of infiltration rates in Table 4, the performance of the infiltration models on the plain surface at the higher temperature range was in the order KO > HO > MK > PH > SM > SCS.

Initial infiltration rates were majorly dependent on soil structure and antecedent moisture content, and hence did not show a significant trend for slope and temperature variations. All the chosen infiltration models were efficient for estimating infiltration rate and cumulative infiltration in the lower temperature ranges on the plain surface (standard situation) compared to the other scenarios. The competence was least for higher temperatures and the inclined surface (combined effect of slope and temperature). Statistical analysis showed that the KO model performed relatively better than the others in estimating infiltration rate and volume when temperature or slope increased.

Table 4. Statistical comparison of parameters of selected models for infiltration rate estimation on different slope and temperature ranges in Okhla landfill

Model	Parameters		Statistical parameters				Mean temperature (°C)	Slope (°)
	$\alpha/S/k$	β	R^2	RSE	PBIAS	NSE		
Kostiakov	0.100	0.439	0.917	0.178	–0.050	0.968	29	4
Modified Kostiakov	0.111	0.736	0.966	0.163	0.022	0.973		
Horton	0.693	NA	0.946	0.378	–0.299	0.857		
Smith	0.114	0.729	0.984	0.183	0.063	0.966		
SCS	0.140	0.600	0.976	0.326	0.096	0.894		
Philip	0.155	0.011	0.987	0.225	–0.010	0.949		
Kostiakov	0.225	0.390	0.934	0.290	0.010	0.913	38	4
Modified Kostiakov	0.190	0.450	0.920	0.308	0.009	0.906		
Horton	0.070	NA	0.995	0.131	–0.098	0.983		
Smith	0.200	0.465	0.913	0.326	0.106	0.894		
SCS	0.250	0.444	0.919	0.399	0.017	0.841		
Philip	0.354	0.030	0.901	0.332	0.000	0.890		
Kostiakov	0.337	0.525	0.982	0.189	0.019	0.964	33	23
Modified Kostiakov	0.320	0.650	0.966	0.250	–0.010	0.937		
Horton	0.300	NA	0.953	0.357	–0.282	0.873		
Smith	0.298	0.670	0.963	0.245	–0.088	0.940		
SCS	0.337	0.525	0.982	0.189	0.019	0.964		
Philip	0.370	0.020	0.985	0.392	–0.246	0.846		
Kostiakov	0.479	0.375	0.936	0.296	0.013	0.912	39	23
Modified Kostiakov	0.365	0.380	0.934	0.243	–0.004	0.941		
Horton	0.120	NA	0.974	0.326	–0.232	0.894		
Smith	0.370	0.420	0.923	0.266	–0.034	0.929		
SCS	0.450	0.360	0.940	0.258	–0.026	0.934		
Philip	0.800	0.065	0.900	0.332	0.008	0.890		

Note: (a) Temperature ranges from 26°C to 32°C and 30°C to 35°C (experiment in morning/forenoon session). (b) Temperature ranges from 36°C to 42°C and 38°C to 42°C (experiment in the afternoon session). (c) S is the sorptivity for the Philip model and k the decay coefficient for the Horton model. (d) α and β are the multiplying and exponent parameters respectively.

Discussion

Temperature variation is a significant factor in the infiltration mechanism in the solid waste bulk due to exothermic reactions in the complex system[36]. The infiltration rate in the afternoon experimental session was higher than that observed in the morning session on the plain surfaces (Figure 4), which can be justified considering soil temperature as a function of the infiltration process[32]. As the temperature increases, more thermal movement of water molecules is anticipated, thus reducing the relative mutual friction, which helps in the qualitative clarification of the reduction in viscosity and increment in hydraulic conductivity at higher temperatures[37]. Therefore, an increment in temperature increases the infiltration rate and volume in the experiments conducted at a relatively higher temperature range[16]. Hydraulic conductivity of the local soil was proven to be the most relevant aspect of the infiltration process[38].

The solid waste in the Okhla landfill was dumped and covered by soil in a layer-on-layer structure, which created a higher possibility of subsurface flow depending on the macro–micropores distribution in the soil matrix. The infiltration rate was higher for the inclined surface than the plain surface due to an increment in the lateral component of flow from the macropores for higher inclination, which increased the gravitational potential[39]. The water infiltrated from the top layer, entering the vertical direction and flowing through the inclined permeable surface due to gravitational force[40]. The amount of infiltrated water was significantly higher on an inclined surface in the afternoon than on the plain surface in the morning due to the combined effect of slope and higher temperature. Previous experimental studies have observed similar results due to rill erosion on the thin soil crust[41]. In addition, results from theoretical formulation using Green–Ampt and Richard equations have presented similar trends under ponded water conditions[42].

Model analysis revealed that all focused classical models have a problem overestimating the infiltrated volume on the inclined surface with a higher temperature range. The model overestimation resulted from the influence of varying depths of compacted earth cover on solid waste. The average infiltrated volume was approximately three times higher on inclined surfaces, possibly due to thinning of the covering layer on such surfaces. Liu *et al.*[43] observed similar overestimated outcomes using the Hydraulic bureau's equation which used to calculate the steady-state infiltration rate in paddy fields and Chen and Lee's equation for alluvial soil and brown soil in paddy fields. Another reason for overestimation could be the assumptions of homogeneous soil properties and constant moisture content throughout the surface[44].

The performance evaluation was based on estimating infiltration rate, cumulative infiltration, and overall assessment

for all the scenarios mentioned above. The KO and MK models were the most efficient for estimating infiltration rate and cumulative infiltration respectively. The KO model was best suited for assessing plain and inclined surfaces at lower and higher temperatures. Multiplying parameter of the KO infiltration model showed an increasing trend with slope and temperature increment. The same model parameter was increased at a higher rate for experiments under the combined effects of temperature and slope. The exponent parameter of the KO model did not show any correlation with the variations, although the values were within the range as demonstrated through previous experimental studies[12,45,46]. The multiplying parameters of the SCS model showed a similar increasing trend with an increment in the chosen physical features; however, the exponent showed a negative trend with the increment in slope and temperature. Zolfaghari *et al.*[45] have reported similar results for the SCS model parameters on a plain surface.

The decay coefficient of the HO model showed a negative trend with focused factors. The PH model did not perform efficiently in the experiments, except for estimating cumulative infiltration in the 23° inclined surface at a higher temperature. However, in the PH model, the additive parameter showed a negative correlation. Sorptivity was correlated positively with temperature due to a reduction in surface tension and viscosity of water with an increase in temperature, resulting increased sorptivity[47]. The range of sorptivity for the standard scenario was found to be within the values estimated by Zolfaghari *et al.*[45] and Farid *et al.*[46]. The limiting value of sorptivity was analysed as 0.80 for the experimental data under the combined impact of inclined surface and high temperature. The multiplying parameter of the MK model showed a similar increasing trend with slope and temperature and agreed with the experimental assessment of the MK model by Zolfaghari *et al.*[45] on a plain surface.

Conclusion

A comparative analysis of the infiltration process was done for an inclined surface and temperature variation in the Okhla landfill based on ring-infiltrometer experimental data. The data showed an increment in cumulative infiltration for the higher temperature range and higher surface inclination for ponded water. The order of performance of classical models for estimating infiltration rates in all four scenarios was MK > KO > SCS > SM > HO > PH. The efficiency of the models for estimating the infiltrated volume in decreasing order was KO > SCS > MK > HO > SM > PH. Overall, the KO model showed the most efficient performance for estimating infiltration rate and infiltrated volume by generating the simulated outcomes closest to the observation data, considering the temperature and slope variation. The recommended range of multiplying constant and exponent parameters of the KO model is 0.10–0.48 and 0.38–0.74 respectively, for a given range of slope and temperature. This study will help select the best suitable model and range of parameters to incorporate the effects of temperature and slope to simulate the infiltration process. Due to spatial variability, the parameters would be required to redefine the above-mentioned models for a heterogeneous system on a larger scale.

Conflict of interest: The authors declare no conflict of interest.

Data availability statement: The raw/processed datasets generated and/or analysed in the present study are not publicly available, but can be obtained from the corresponding author on reasonable request.

1. Singh, R. P., Tyagi, V. V., Allen, T., Ibrahim, M. H. and Kothari, R., An overview for exploring the possibilities of energy generation from municipal solid waste (MSW) in Indian scenar*io. Renew. Sustain. Energy Rev*., 2011, **15**, 4797–4808; https://doi.org/10.1016/J.RSER.2011.07.071.
2. Census of India 2011, Population projections for India and the states: 2011–2036, National Commission on Population, Ministry of Health & Family Welfare, New Delhi, 2020.
3. Annual Report with respect to solid waste management rules, 2016 in respect of NCT of Delhi for the Year 2016, Delhi Pollution Control Committee, Government of NCT of Delhi, New Delhi, 2019.
4. Annual Report in respect of NCT of Delhi for the year 2021–2022 on the implementation of solid waste management rules, 2016, New Delhi, 2022.
5. Delhi Pollution Control Council, Compliance report of Govt. of NCT of Delhi in OA No. 606/2018, New Delhi, 2020.
6. Talyan, V., Dahiya, R. P. and Sreekrishnan, T. R., State of municipal solid waste management in Delhi, the capital of India. *Waste Manage.*, 2008, **28**, 1276–1287.
7. Chakma, S. and Mathur, S., Estimation of primary and mechanical compression in MSW landfills. *J. Hazard., Toxic, Radioact. Waste*, 2012, **16**, 298–303.
8. Mukherjee, S., Mukhopadhyay, S., Hashim, M. A. and Sen Gupta, B., Contemporary environmental issues of landfill leachate: assessment and remedies. *Crit. Rev. Environ. Sci. Technol*., 2014, **45**, 472–590; https://doi.org/10.1080/10643389.2013.876524.
9. Chakma, S. and Mathur, S., Postclosure long-term settlement for MSW landfills. *J. Hazard., Toxic, Radioact. Waste*, 2013, **17**, 81–88.
10. Hopmans, J., Clausnitzer, V. and Kosugi, K. I., Evaluation of various infiltration models. *Sci. Agric.*, 1995, **140**, 5–8.
11. Haghighi, F., Gorji, M., Shorafa, M., Sarmadian, F. and Mohammadi, M. H., Evaluation of some infiltration models and hydraulic parameters. *Span. J. Agric. Res.*, 2010, **8**, 210.
12. Sihag, P., Tiwari, N. K. and Ranjan, S., Estimation and inter-comparison of infiltration models. *Water Sci.*, 2017, **31**, 34–43.
13. Helalia, A. M., The relation between soil infiltration and effective porosity in different soils. *Agric. Water Manage.*, 1993, **24**, 39–47.
14. Mishra, S. K., Tyagi, J. V. and Singh, V. P., Comparison of infiltration models. *Hydrol. Process.*, 2003, **17**, 2629–2652.
15. Skaggs, R. W., Huggins, L., Monke, E. and Foster, G., Experimental evaluation of infiltration equations. *Trans. ASAE*, 1969, **12**, 822–828.
16. Levy, G. J., Smith, H. J. C. and Agassi, M., Water temperature effect on hydraulic conductivity and infiltration rate of soils. *S. Afr. J. Plant Soil*, 1989, **6**, 240–244.
17. Gavin, K. and Xue, J., A simple method to analyze infiltration into unsaturated soil slopes. *Comput. Geotech.*, 2008, **35**, 223–230.
18. Langhans, C., Govers, G. and Diels, J., Development and parameterization of an infiltration model accounting for water depth and rainfall intensity. *Hydrol. Process.*, 2013, **27**, 3777–3790.

19. Avudainayagam, S., Sharma, K. K. and Rajamani, V., Rate of infiltration – an *in situ* measurement. *Curr. Sci.*, 1987, **13**, 663–664.
20. Fenn, D. G., Hanley, K. J. and Degeare, T. V., Use of the water-balance method for predicting leachate generation from solid-waste-disposal sites. Technical Report, Office of Scientific and Technical Information, US Department of Energy, Washington, DC, USA, 1975; https://www.osti.gov/biblio/6328350
21. Kargas, G. and Kerkides, P., A contribution to the study of the phenomenon of horizontal infiltration. *Water Resour. Manage.*, 2010, **25**, 1131–1141.
22. ICAR, Daily weather data, Indian Council of Agricultural Research, New Delhi, 2020.
23. Mohan, M. and Kandya, A., Impact of urbanization and land-use/land-cover change on diurnal temperature range: a case study of tropical urban airshed of India using remote sensing data. *Sci. Total Environ.*, 2015, **506**–**507**, 453–465.
24. Integrated Research and Action for Development, Report on assessment of landfill gas and pre feasibility study at the Okhla landfill gas utilization as domestic fuel, New Delhi, 2009.
25. Gregory, J. H., Dukes, M. D., Miller, G. L. and Jones, P. H., Analysis of double-ring infiltration techniques and development of a simple automatic water delivery system. *Appl. Turfgrass Sci.*, 2005, **2**, 1–7.
26. ASTM D3385-03, Standard test method for infiltration rate of soils in field using double-ring infiltrometer, ASTM International, 2009.
27. Rocheta, V. L. S., Isidoro, J. M. G. P. and de Lima, J. L. M. P., Infiltration of Portuguese cobblestone pavements – an exploratory assessment using a double-ring infiltrometer. *Urban Water J.*, 2015, **14**, 291–297; http://dx.doi.org/10.1080/1573062X.2015.1111914.
28. Shukla, M. K., Lal, R., Owens, L. B. and Unkefer, P., Land use and management impacts on structure and infiltration characteristics of soils in the North Appalachian region of Ohio. *Soil Sci.*, 2003, **168**, 167–177.
29. Kirkham, M. B. (ed.), Infiltration. In *Principals of Soil Plant Water Relations (Second Edition)*, 2014, pp. 201–227.
30. Legates, D. R. and McCabe, G. J., Evaluating the use of 'goodness-of-fit' measures in hydrologic and hydroclimatic model validation. *Water Resour. Res.*, 1999, **35**, 233–241.
31. Moriasi, D. N., Arnold, J. G., Van, L., Bingner, W., Harmel, R. D. and Veith, T. L., Model evaluation guidelines for systematic quantification of accuracy in watershed simulations. *Trans. ASABE*, 2007, **50**, 885–900.
32. Jaynes, D. B., Temperature variations effect on field-measured infiltration. *Soil Sci. Soc. Am. J.*, 1990, **54**, 305–312.
33. Sharma, K. D., Singh, H. P. and Pareek, O. P., Rainwater infiltration into a bare loamy sand. *Hydrol. Sci. J.*, 2009, **28**, 417–424; https://doi.org/10.1080/02626668309491980.
34. Mu, W. *et al.*, Effects of rainfall intensity and slope gradient on runoff and soil moisture content on different growing stages of spring maize. *Water*, 2015, **7**, 2990–3008.
35. Khan, M. N. *et al.*, Effect of slope, rainfall intensity and mulch on erosion and infiltration under simulated rain on purple soil of south-western Sichuan Province, China. *Water*, 2016, **8**, 528.
36. Klein, R., Baumann, T., Kahapka, E. and Niessner, R., Temperature development in a modern municipal solid waste incineration (MSWI) bottom ash landfill with regard to sustainable waste management. *J. Hazard. Mater.*, 2001, **83**, 265–280.
37. Wright, P. G., The variation of viscosity with temperature. *Phys. Educ.*, 1977, **12**, 323–325.
38. Petrucci, G., De Bondt, K. and Claeys, P., Toward better practices in infiltration regulations for urban stormwater management. *Urban Water J.*, 2016, **14**, 546–550.
39. Lv, M., Hao, Z., Liu, Z. and Yu, Z., Conditions for lateral downslope unsaturated flow and effects of slope angle on soil moisture movement. *J. Hydrol.*, 2013, **486**, 321–333.
40. Miyazaki, T., *Water Flow in Soils*, Boca Raton, CRC Press, 2005, pp. 163–217.
41. Poesen, J., The influence of slope angle on infiltration rate and Hortonian overland flow volume. *Z. Geomorphol. Suppl.*, 1984, **49**, 117–131.
42. Chen, L. and Young, M. H., Green–Ampt infiltration model for sloping surfaces. *Water Resour. Res.*, 2006, **42**, 1–9.
43. Liu, C.-W., Chen, S.-K., Jou, S.-W. and Kuo, S.-F., Estimation of the infiltration rate of a paddy field in Yun-Lin, Taiwan. *Agric. Syst.*, 2001, **1**, 41–54.
44. Chahinian, N., Moussa, R., Andrieux, P. and Voltz, M., Comparison of infiltration models to simulate flood events at the field scale. *J. Hydrol.*, 2005, **306**, 191–214.
45. Zolfaghari, A. A., Mirzaee, S. and Gorji, M., Comparison of different models for estimating cumulative infiltration. *Int. J. Soil Sci.*, 2012, **7**, 108–115.
46. Farid, H. U. *et al.*, Estimation of infiltration model parameters and their comparison to simulate the onsite soil infiltration characteristics. *Int. J. Agric. Biol. Eng.*, 2019, **12**, 84–91.
47. Ioannou, I., Charalambous, C. and Hall, C., The temperature variation of the water sorptivity of construction materials. *Mater. Struct. Constr.*, 2017, **50**, 1–12.

Received 12 June 2021; revised accepted 29 September 2022

doi: 10.18520/cs/v124/i1/94-101